Fermilab-Pub-06/257-E

Search for W' boson production in the $W' \to t\bar{b}$ decay channel

V.M. Abazov,[36] B. Abbott,[76] M. Abolins,[66] B.S. Acharya,[29] M. Adams,[52] T. Adams,[50] M. Agelou,[18] J.-L. Agram,[19] S.H. Ahn,[31] M. Ahsan,[60] G.D. Alexeev,[36] G. Alkhazov,[40] A. Alton,[65] G. Alverson,[64] G.A. Alves,[2] M. Anastasoaie,[35] T. Andeen,[54] S. Anderson,[46] B. Andrieu,[17] M.S. Anzelc,[54] Y. Arnoud,[14] M. Arov,[53] A. Askew,[50] B. Åsman,[41] A.C.S. Assis Jesus,[3] O. Atramentov,[58] C. Autermann,[21] C. Avila,[8] C. Ay,[24] F. Badaud,[13] A. Baden,[62] L. Bagby,[53] B. Baldin,[51] D.V. Bandurin,[60] P. Banerjee,[29] S. Banerjee,[29] E. Barberis,[64] P. Bargassa,[81] P. Baringer,[59] C. Barnes,[44] J. Barreto,[2] J.F. Bartlett,[51] U. Bassler,[17] D. Bauer,[44] A. Bean,[59] M. Begalli,[3] M. Begel,[72] C. Belanger-Champagne,[5] L. Bellantoni,[51] A. Bellavance,[68] J.A. Benitez,[66] S.B. Beri,[27] G. Bernardi,[17] R. Bernhard,[42] L. Berntzon,[15] I. Bertram,[43] M. Besançon,[18] R. Beuselinck,[44] V.A. Bezzubov,[39] P.C. Bhat,[51] V. Bhatnagar,[27] M. Binder,[25] C. Biscarat,[43] K.M. Black,[63] I. Blackler,[44] G. Blazey,[53] F. Blekman,[44] S. Blessing,[50] D. Bloch,[19] K. Bloom,[68] U. Blumenschein,[23] A. Boehnlein,[51] O. Boeriu,[56] T.A. Bolton,[60] G. Borissov,[43] K. Bos,[34] E.E. Boos,[38] T. Bose,[78] A. Brandt,[79] R. Brock,[66] G. Brooijmans,[71] A. Bross,[51] D. Brown,[79] N.J. Buchanan,[50] D. Buchholz,[54] M. Buehler,[82] V. Buescher,[23] V. Bunichev,[38] S. Burdin,[51] S. Burke,[46] T.H. Burnett,[83] E. Busato,[17] C.P. Buszello,[44] J.M. Butler,[63] P. Calfayan,[25] S. Calvet,[15] J. Cammin,[72] S. Caron,[34] W. Carvalho,[3] B.C.K. Casey,[78] N.M. Cason,[56] H. Castilla-Valdez,[33] S. Chakrabarti,[29] D. Chakraborty,[53] K.M. Chan,[72] A. Chandra,[49] D. Chapin,[78] F. Charles,[19] E. Cheu,[46] F. Chevallier,[14] D.K. Cho,[63] S. Choi,[32] B. Choudhary,[28] L. Christofek,[59] D. Claes,[68] B. Clément,[19] C. Clément,[41] Y. Coadou,[5] M. Cooke,[81] W.E. Cooper,[51] D. Coppage,[59] M. Corcoran,[81] M.-C. Cousinou,[15] B. Cox,[45] S. Crépé-Renaudin,[14] D. Cutts,[78] M. Ćwiok,[30] H. da Motta,[2] A. Das,[63] M. Das,[61] B. Davies,[43] G. Davies,[44] G.A. Davis,[54] K. De,[79] P. de Jong,[34] S.J. de Jong,[35] E. De La Cruz-Burelo,[65] C. De Oliveira Martins,[3] J.D. Degenhardt,[65] F. Déliot,[18] M. Demarteau,[51] R. Demina,[72] P. Demine,[18] D. Denisov,[51] S.P. Denisov,[39] S. Desai,[73] H.T. Diehl,[51] M. Diesburg,[51] M. Doidge,[43] A. Dominguez,[68] H. Dong,[73] L.V. Dudko,[38] L. Duflot,[16] S.R. Dugad,[29] A. Duperrin,[15] J. Dyer,[66] A. Dyshkant,[53] M. Eads,[68] D. Edmunds,[66] T. Edwards,[45] J. Ellison,[49] J. Elmsheuser,[25] V.D. Elvira,[51] S. Eno,[62] P. Ermolov,[38] J. Estrada,[51] H. Evans,[55] A. Evdokimov,[37] V.N. Evdokimov,[39] S.N. Fatakia,[63] L. Feligioni,[63] A.V. Ferapontov,[60] T. Ferbel,[72] F. Fiedler,[25] F. Filthaut,[35] W. Fisher,[51] H.E. Fisk,[51] I. Fleck,[23] M. Ford,[45] M. Fortner,[53] H. Fox,[23] S. Fu,[51] S. Fuess,[51] T. Gadfort,[83] C.F. Galea,[35] E. Gallas,[51] E. Galyaev,[56] C. Garcia,[72] A. Garcia-Bellido,[83] J. Gardner,[59] V. Gavrilov,[37] A. Gay,[19] P. Gay,[13] D. Gelé,[19] R. Gelhaus,[49] C.E. Gerber,[52] Y. Gershtein,[50] D. Gillberg,[5] G. Ginther,[72] N. Gollub,[41] B. Gómez,[8] A. Goussiou,[56] P.D. Grannis,[73] H. Greenlee,[51] Z.D. Greenwood,[61] E.M. Gregores,[4] G. Grenier,[20] Ph. Gris,[13] J.-F. Grivaz,[16] S. Grünendahl,[51] M.W. Grünewald,[30] F. Guo,[73] J. Guo,[73] G. Gutierrez,[51] P. Gutierrez,[76] A. Haas,[71] N.J. Hadley,[62] P. Haefner,[25] S. Hagopian,[50] J. Haley,[69] I. Hall,[76] R.E. Hall,[48] L. Han,[7] K. Hanagaki,[51] K. Harder,[60] A. Harel,[72] R. Harrington,[64] J.M. Hauptman,[58] R. Hauser,[66] J. Hays,[54] T. Hebbeker,[21] D. Hedin,[53] J.G. Hegeman,[34] J.M. Heinmiller,[52] A.P. Heinson,[49] U. Heintz,[63] C. Hensel,[59] G. Hesketh,[64] M.D. Hildreth,[56] R. Hirosky,[82] J.D. Hobbs,[73] B. Hoeneisen,[12] H. Hoeth,[26] M. Hohlfeld,[16] S.J. Hong,[31] R. Hooper,[78] P. Houben,[34] Y. Hu,[73] Z. Hubacek,[10] V. Hynek,[9] I. Iashvili,[70] R. Illingworth,[51] A.S. Ito,[51] S. Jabeen,[63] M. Jaffré,[16] S. Jain,[76] K. Jakobs,[23] C. Jarvis,[62] A. Jenkins,[44] R. Jesik,[44] K. Johns,[46] C. Johnson,[71] M. Johnson,[51] A. Jonckheere,[51] P. Jonsson,[44] A. Juste,[51] D. Käfer,[21] S. Kahn,[74] E. Kajfasz,[15] A.M. Kalinin,[36] J.M. Kalk,[61] J.R. Kalk,[66] S. Kappler,[21] D. Karmanov,[38] J. Kasper,[63] P. Kasper,[51] I. Katsanos,[71] D. Kau,[50] R. Kaur,[27] R. Kehoe,[80] S. Kermiche,[15] S. Kesisoglou,[78] N. Khalatyan,[63] A. Khanov,[77] A. Kharchilava,[70] Y.M. Kharzheev,[36] D. Khatidze,[71] H. Kim,[79] T.J. Kim,[31] M.H. Kirby,[35] B. Klima,[51] J.M. Kohli,[27] J.-P. Konrath,[23] M. Kopal,[76] V.M. Korablev,[39] J. Kotcher,[74] B. Kothari,[71] A. Koubarovsky,[38] A.V. Kozelov,[39] J. Kozminski,[66] D. Krop,[55] A. Kryemadhi,[82] T. Kuhl,[24] A. Kumar,[70] S. Kunori,[62] A. Kupco,[11] T. Kurča,[20,*] J. Kvita,[9] S. Lager,[41] S. Lammers,[71] G. Landsberg,[78] J. Lazoflores,[50] A.-C. Le Bihan,[19] P. Lebrun,[20] W.M. Lee,[53] A. Leflat,[38] F. Lehner,[42] V. Lesne,[13] J. Leveque,[46] P. Lewis,[44] J. Li,[79] Q.Z. Li,[51] J.G.R. Lima,[53] D. Lincoln,[51] J. Linnemann,[66] V.V. Lipaev,[39] R. Lipton,[51] Z. Liu,[5] L. Lobo,[44] A. Lobodenko,[40] M. Lokajicek,[11] A. Lounis,[19] P. Love,[43] H.J. Lubatti,[83] M. Lynker,[56] A.L. Lyon,[51] A.K.A. Maciel,[2] R.J. Madaras,[47] P. Mättig,[26] C. Magass,[21] A. Magerkurth,[65] A.-M. Magnan,[14] N. Makovec,[16] P.K. Mal,[56] H.B. Malbouisson,[3] S. Malik,[68] V.L. Malyshev,[36] H.S. Mao,[6] Y. Maravin,[60] M. Martens,[51] S.E.K. Mattingly,[78] R. McCarthy,[73] D. Meder,[24] A. Melnitchouk,[67] A. Mendes,[15] L. Mendoza,[8] M. Merkin,[38] K.W. Merritt,[51] A. Meyer,[21] J. Meyer,[22] M. Michaut,[18] H. Miettinen,[81] T. Millet,[20] J. Mitrevski,[71] J. Molina,[3] N.K. Mondal,[29]

J. Monk,[45] R.W. Moore,[5] T. Moulik,[59] G.S. Muanza,[16] M. Mulders,[51] M. Mulhearn,[71] L. Mundim,[3] Y.D. Mutaf,[73] E. Nagy,[15] M. Naimuddin,[28] M. Narain,[63] N.A. Naumann,[35] H.A. Neal,[65] J.P. Negret,[8] S. Nelson,[50] P. Neustroev,[40] C. Noeding,[23] A. Nomerotski,[51] S.F. Novaes,[4] T. Nunnemann,[25] V. O'Dell,[51] D.C. O'Neil,[5] G. Obrant,[40] V. Oguri,[3] N. Oliveira,[3] N. Oshima,[51] R. Otec,[10] G.J. Otero y Garzón,[52] M. Owen,[45] P. Padley,[81] N. Parashar,[57] S.-J. Park,[72] S.K. Park,[31] J. Parsons,[71] R. Partridge,[78] N. Parua,[73] A. Patwa,[74] G. Pawloski,[81] P.M. Perea,[49] E. Perez,[18] M. Perfilov,[38] K. Peters,[45] P. Pétroff,[16] M. Petteni,[44] R. Piegaia,[1] M.-A. Pleier,[22] P.L.M. Podesta-Lerma,[33] V.M. Podstavkov,[51] Y. Pogorelov,[56] M.-E. Pol,[2] A. Pompoš,[76] B.G. Pope,[66] A.V. Popov,[39] W.L. Prado da Silva,[3] H.B. Prosper,[50] S. Protopopescu,[74] J. Qian,[65] A. Quadt,[22] B. Quinn,[67] K.J. Rani,[29] K. Ranjan,[28] P.N. Ratoff,[43] P. Renkel,[80] S. Reucroft,[64] M. Rijssenbeek,[73] I. Ripp-Baudot,[19] F. Rizatdinova,[77] S. Robinson,[44] R.F. Rodrigues,[3] C. Royon,[18] P. Rubinov,[51] R. Ruchti,[56] V.I. Rud,[38] G. Sajot,[14] A. Sánchez-Hernández,[33] M.P. Sanders,[62] A. Santoro,[3] G. Savage,[51] L. Sawyer,[61] T. Scanlon,[44] D. Schaile,[25] R.D. Schamberger,[73] Y. Scheglov,[40] H. Schellman,[54] P. Schieferdecker,[25] C. Schmitt,[26] C. Schwanenberger,[45] A. Schwartzman,[69] R. Schwienhorst,[66] S. Sengupta,[50] H. Severini,[76] E. Shabalina,[52] M. Shamim,[60] V. Shary,[18] A.A. Shchukin,[39] W.D. Shephard,[56] R.K. Shivpuri,[28] D. Shpakov,[51] V. Siccardi,[19] R.A. Sidwell,[60] V. Simak,[10] V. Sirotenko,[51] P. Skubic,[76] P. Slattery,[72] R.P. Smith,[51] G.R. Snow,[68] J. Snow,[75] S. Snyder,[74] S. Söldner-Rembold,[45] X. Song,[53] L. Sonnenschein,[17] A. Sopczak,[43] M. Sosebee,[79] K. Soustruznik,[9] M. Souza,[2] B. Spurlock,[79] J. Stark,[14] J. Steele,[61] V. Stolin,[37] A. Stone,[52] D.A. Stoyanova,[39] J. Strandberg,[41] M.A. Strang,[70] M. Strauss,[76] R. Ströhmer,[25] D. Strom,[54] M. Strovink,[47] L. Stutte,[51] S. Sumowidagdo,[50] A. Sznajder,[3] M. Talby,[15] P. Tamburello,[46] W. Taylor,[5] P. Telford,[45] J. Temple,[46] B. Tiller,[25] M. Titov,[23] V.V. Tokmenin,[36] M. Tomoto,[51] T. Toole,[62] I. Torchiani,[23] S. Towers,[43] T. Trefzger,[24] S. Trincaz-Duvoid,[17] D. Tsybychev,[73] B. Tuchming,[18] C. Tully,[69] A.S. Turcot,[45] P.M. Tuts,[71] R. Unalan,[66] L. Uvarov,[40] S. Uvarov,[40] S. Uzunyan,[53] B. Vachon,[5] P.J. van den Berg,[34] R. Van Kooten,[55] W.M. van Leeuwen,[34] N. Varelas,[52] E.W. Varnes,[46] A. Vartapetian,[79] I.A. Vasilyev,[39] M. Vaupel,[26] P. Verdier,[20] L.S. Vertogradov,[36] M. Verzocchi,[51] F. Villeneuve-Seguier,[44] P. Vint,[44] J.-R. Vlimant,[17] E. Von Toerne,[60] M. Voutilainen,[68,†] M. Vreeswijk,[34] H.D. Wahl,[50] L. Wang,[62] J. Warchol,[56] G. Watts,[83] M. Wayne,[56] M. Weber,[51] H. Weerts,[66] N. Wermes,[22] M. Wetstein,[62] A. White,[79] D. Wicke,[26] G.W. Wilson,[59] S.J. Wimpenny,[49] M. Wobisch,[51] J. Womersley,[51] D.R. Wood,[64] T.R. Wyatt,[45] Y. Xie,[78] N. Xuan,[56] S. Yacoob,[54] R. Yamada,[51] M. Yan,[62] T. Yasuda,[51] Y.A. Yatsunenko,[36] K. Yip,[74] H.D. Yoo,[78] S.W. Youn,[54] C. Yu,[14] J. Yu,[79] A. Yurkewicz,[73] A. Zatserklyaniy,[53] C. Zeitnitz,[26] D. Zhang,[51] T. Zhao,[83] B. Zhou,[65] J. Zhu,[73] M. Zielinski,[72] D. Zieminska,[55] A. Zieminski,[55] V. Zutshi,[53] and E.G. Zverev[38]

(DØ Collaboration)

[1] *Universidad de Buenos Aires, Buenos Aires, Argentina*
[2] *LAFEX, Centro Brasileiro de Pesquisas Físicas, Rio de Janeiro, Brazil*
[3] *Universidade do Estado do Rio de Janeiro, Rio de Janeiro, Brazil*
[4] *Instituto de Física Teórica, Universidade Estadual Paulista, São Paulo, Brazil*
[5] *University of Alberta, Edmonton, Alberta, Canada, Simon Fraser University, Burnaby, British Columbia, Canada, York University, Toronto, Ontario, Canada, and McGill University, Montreal, Quebec, Canada*
[6] *Institute of High Energy Physics, Beijing, People's Republic of China*
[7] *University of Science and Technology of China, Hefei, People's Republic of China*
[8] *Universidad de los Andes, Bogotá, Colombia*
[9] *Center for Particle Physics, Charles University, Prague, Czech Republic*
[10] *Czech Technical University, Prague, Czech Republic*
[11] *Center for Particle Physics, Institute of Physics, Academy of Sciences of the Czech Republic, Prague, Czech Republic*
[12] *Universidad San Francisco de Quito, Quito, Ecuador*
[13] *Laboratoire de Physique Corpusculaire, IN2P3-CNRS, Université Blaise Pascal, Clermont-Ferrand, France*
[14] *Laboratoire de Physique Subatomique et de Cosmologie, IN2P3-CNRS, Universite de Grenoble 1, Grenoble, France*
[15] *CPPM, IN2P3-CNRS, Université de la Méditerranée, Marseille, France*
[16] *IN2P3-CNRS, Laboratoire de l'Accélérateur Linéaire, Orsay, France*
[17] *LPNHE, IN2P3-CNRS, Universités Paris VI and VII, Paris, France*
[18] *DAPNIA/Service de Physique des Particules, CEA, Saclay, France*
[19] *IPHC, IN2P3-CNRS, Université Louis Pasteur, Strasbourg, France, and Université de Haute Alsace, Mulhouse, France*
[20] *Institut de Physique Nucléaire de Lyon, IN2P3-CNRS, Université Claude Bernard, Villeurbanne, France*
[21] *III. Physikalisches Institut A, RWTH Aachen, Aachen, Germany*
[22] *Physikalisches Institut, Universität Bonn, Bonn, Germany*
[23] *Physikalisches Institut, Universität Freiburg, Freiburg, Germany*
[24] *Institut für Physik, Universität Mainz, Mainz, Germany*
[25] *Ludwig-Maximilians-Universität München, München, Germany*
[26] *Fachbereich Physik, University of Wuppertal, Wuppertal, Germany*

[27] *Panjab University, Chandigarh, India*
[28] *Delhi University, Delhi, India*
[29] *Tata Institute of Fundamental Research, Mumbai, India*
[30] *University College Dublin, Dublin, Ireland*
[31] *Korea Detector Laboratory, Korea University, Seoul, Korea*
[32] *SungKyunKwan University, Suwon, Korea*
[33] *CINVESTAV, Mexico City, Mexico*
[34] *FOM-Institute NIKHEF and University of Amsterdam/NIKHEF, Amsterdam, The Netherlands*
[35] *Radboud University Nijmegen/NIKHEF, Nijmegen, The Netherlands*
[36] *Joint Institute for Nuclear Research, Dubna, Russia*
[37] *Institute for Theoretical and Experimental Physics, Moscow, Russia*
[38] *Moscow State University, Moscow, Russia*
[39] *Institute for High Energy Physics, Protvino, Russia*
[40] *Petersburg Nuclear Physics Institute, St. Petersburg, Russia*
[41] *Lund University, Lund, Sweden, Royal Institute of Technology and Stockholm University, Stockholm, Sweden, and Uppsala University, Uppsala, Sweden*
[42] *Physik Institut der Universität Zürich, Zürich, Switzerland*
[43] *Lancaster University, Lancaster, United Kingdom*
[44] *Imperial College, London, United Kingdom*
[45] *University of Manchester, Manchester, United Kingdom*
[46] *University of Arizona, Tucson, Arizona 85721, USA*
[47] *Lawrence Berkeley National Laboratory and University of California, Berkeley, California 94720, USA*
[48] *California State University, Fresno, California 93740, USA*
[49] *University of California, Riverside, California 92521, USA*
[50] *Florida State University, Tallahassee, Florida 32306, USA*
[51] *Fermi National Accelerator Laboratory, Batavia, Illinois 60510, USA*
[52] *University of Illinois at Chicago, Chicago, Illinois 60607, USA*
[53] *Northern Illinois University, DeKalb, Illinois 60115, USA*
[54] *Northwestern University, Evanston, Illinois 60208, USA*
[55] *Indiana University, Bloomington, Indiana 47405, USA*
[56] *University of Notre Dame, Notre Dame, Indiana 46556, USA*
[57] *Purdue University Calumet, Hammond, Indiana 46323, USA*
[58] *Iowa State University, Ames, Iowa 50011, USA*
[59] *University of Kansas, Lawrence, Kansas 66045, USA*
[60] *Kansas State University, Manhattan, Kansas 66506, USA*
[61] *Louisiana Tech University, Ruston, Louisiana 71272, USA*
[62] *University of Maryland, College Park, Maryland 20742, USA*
[63] *Boston University, Boston, Massachusetts 02215, USA*
[64] *Northeastern University, Boston, Massachusetts 02115, USA*
[65] *University of Michigan, Ann Arbor, Michigan 48109, USA*
[66] *Michigan State University, East Lansing, Michigan 48824, USA*
[67] *University of Mississippi, University, Mississippi 38677, USA*
[68] *University of Nebraska, Lincoln, Nebraska 68588, USA*
[69] *Princeton University, Princeton, New Jersey 08544, USA*
[70] *State University of New York, Buffalo, New York 14260, USA*
[71] *Columbia University, New York, New York 10027, USA*
[72] *University of Rochester, Rochester, New York 14627, USA*
[73] *State University of New York, Stony Brook, New York 11794, USA*
[74] *Brookhaven National Laboratory, Upton, New York 11973, USA*
[75] *Langston University, Langston, Oklahoma 73050, USA*
[76] *University of Oklahoma, Norman, Oklahoma 73019, USA*
[77] *Oklahoma State University, Stillwater, Oklahoma 74078, USA*
[78] *Brown University, Providence, Rhode Island 02912, USA*
[79] *University of Texas, Arlington, Texas 76019, USA*
[80] *Southern Methodist University, Dallas, Texas 75275, USA*
[81] *Rice University, Houston, Texas 77005, USA*
[82] *University of Virginia, Charlottesville, Virginia 22901, USA*
[83] *University of Washington, Seattle, Washington 98195, USA*

(Dated: August 31, 2006)

We present a search for the production of a new heavy gauge boson W' that decays to a top quark and a bottom quark. We have analyzed 230 pb^{-1} of data collected with the DØ detector at the Fermilab Tevatron collider at a center-of-mass energy of 1.96 TeV. No significant excess of

events above the standard model expectation is found in any region of the final state invariant mass distribution. We set upper limits on the production cross section of W' bosons times branching ratio to top quarks at the 95% confidence level for several different W' boson masses. We exclude masses between 200 GeV and 610 GeV for a W' boson with standard-model-like couplings, between 200 GeV and 630 GeV for a W' boson with right-handed couplings that is allowed to decay to both leptons and quarks, and between 200 GeV and 670 GeV for a W' boson with right-handed couplings that is only allowed to decay to quarks.

PACS numbers: 13.85.Rm; 14.70.Pw

The top quark sector offers great potential to look for new physics related to electroweak symmetry breaking. In particular, it is a sensitive probe for the presence of additional gauge bosons beyond those of the standard model (SM). Such new gauge bosons typically arise in extensions to the SM from the presence of additional symmetry groups [1, 2].

Direct searches for the production of additional heavy gauge bosons have focused on the lepton final state of the W' boson decay which has good separation between the W' boson signal and the SM backgrounds. The W' boson lower mass limit in this decay channel is 786 GeV [3]. In these studies, the W' boson is allowed to have right-handed interactions with leptons and quarks, and it is assumed that the right-handed neutrino is lighter than the W' boson. It is also possible that such a W' boson does not interact with leptons and neutrinos but only with quarks. Searching in the quark decay channel avoids assumptions about the mass of a possible right-handed neutrino. Previous direct searches for W' bosons in the quark decay channel have excluded the mass range below 261 GeV [4] and between 300 GeV and 420 GeV [5]. Assuming that the W' boson decays only to quarks and not to leptons yields a lower mass limit of 800 GeV [6]. A search has also been performed in the single top quark final state of the W'-boson decay. Assuming the W' boson has only right-handed interactions and does not decay to leptons, the lower limit on the W' boson mass is 566 GeV [7]. The comprehensive search presented here includes all of these W' boson models. Indirect searches for evidence of a W' boson depend on exactly how it interferes with the SM W boson and the results are thus highly model specific (see Ref. [2] and references therein).

The top quark was discovered in 1995 by the CDF and DØ collaborations [8], but the production of single top quark has not yet been observed. Both collaborations have searched for single top quark production [9, 10, 11, 12, 13]. At the 95% confidence level, the upper limit measured by DØ on the s-channel process is 6.4 pb, and the limit measured by CDF is 13.6 pb. At the same confidence level, the limit on the t-channel production cross section is 5.0 pb from DØ and 10.1 pb from CDF. For comparison, the next-to-leading order (NLO) SM single top quark production cross sections are 0.88 pb in the s-channel and 1.98 pb in the t-channel [14].

The single top quark final state is especially sensitive to the presence of an additional heavy boson, owing to the decay chain $W' \to t\bar{b}$, where the top quark decays to a b quark and a SM W boson. This decay is kinematically allowed as long as the W' mass is larger than the sum of top and bottom quark masses, i.e. as long as it is above about 200 GeV.

An additional heavy boson would appear as a peak in the invariant mass distribution of the $t\bar{b}$ final state. Note that in this letter, the notation $t\bar{b}$ includes both final states $W'^{+} \to t\bar{b}$ and $W'^{-} \to \bar{t}b$. The leading order Feynman diagram for W' boson production resulting in single top quark events is shown in Fig. 1. This diagram is identical to that for SM s-channel single top quark production where the SM W boson appears as the virtual particle [14, 15, 16, 17].

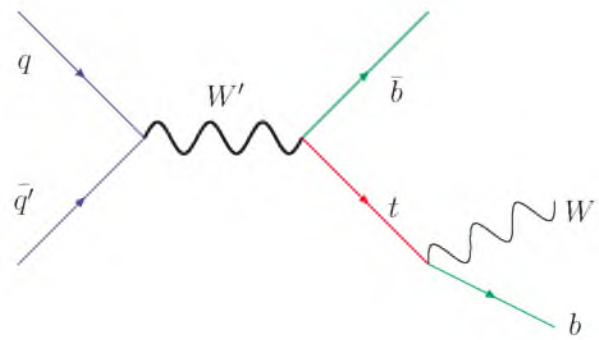

FIG. 1: Leading order Feynman diagram for single top quark production via a heavy W' boson. The top quark decays to a SM W boson and a b quark.

The W' boson also has a t-channel exchange that leads to a single top quark final state. However, the cross section for a t-channel W' process is much smaller than the SM t-channel single top quark production due to the high mass of the W' boson. It will thus not be considered in this letter.

The SM W boson from the top quark decay then decays leptonically or hadronically. A heavy W' boson could also contribute to the top quark decay, but that contribution is negligible, again because of the large W' boson mass, and will not be considered here.

We investigate three models of W' boson production. In each case, we set the CKM mixing matrix elements for the W' boson equal to the SM values. In the first model (W'_L), we make the assumption that the coupling of the W' boson to SM fermions is identical to that of the SM

W boson. Under these assumptions, there is interference between the SM s-channel single top quark process and the W' boson production process from Fig. 1. This interference term is small for large W' boson masses, but it becomes important in the invariant mass range of a few hundred GeV where the SM s-channel production cross section is largest. In our modeling of the W' boson production process, we take this interference into account. This is the first direct search for W' boson production to do so.

In the second and third model (W'_R), the W' boson has only right-handed interactions, hence there is no interference with the SM W boson. In the second model, the W'_R boson is allowed to decay both to leptons and quarks, whereas in the third model it is only allowed to decay to quarks. The main difference between these two models is in the production cross section and the branching fraction to quarks, and we use the same simulated event sample for both models.

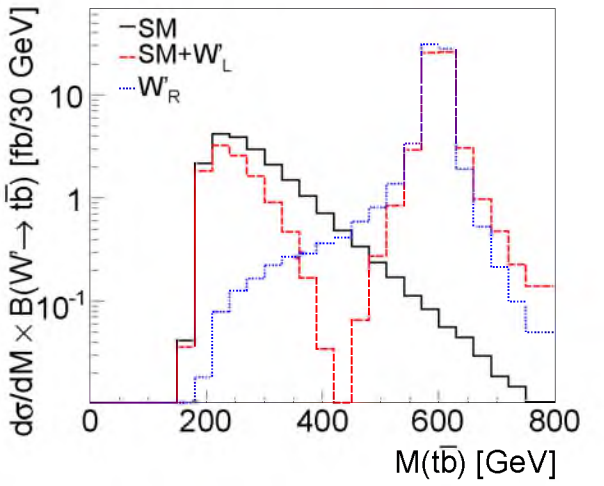

FIG. 2: Histogram of the invariant mass of the top-bottom quark system at the parton level for different models of W' boson production. Shown are the SM s-channel distribution, the $W'_L \to t\bar{b}$ boson distribution, including the interference with the SM contribution, and the $W'_R \to t\bar{b}$ boson contribution, for a W' boson mass of 600 GeV.

Figure 2 compares the invariant mass distribution for the W' models with left-handed coupling (including interference) and right-handed coupling (no interference) with the SM s-channel single top quark distribution. While the position and width of the resonance peak at 600 GeV is not very much affected by the interference, there is significant destructive interference for the left-handed coupling in the invariant mass region between the SM and the resonance peak.

Table I shows the NLO cross sections for single top quark production through a W' boson for the three different models. The cross section for SM-like left-handed W' boson interactions takes into account the W'_L boson contribution, the SM s-channel single top quark contribution, and the interference between them. This combined cross section has been calculated at leading order using CompHEP [18] and then multiplied by the NLO/LO cross section ratio from Table VII of Ref. [2]. The factorization scale has been set equal to the invariant mass of the W' boson. There is no such interference term for right-handed W' boson interactions, and the cross sections in the two right columns of Table I have been taken directly from Ref. [2]. For W'_R boson interactions, the product of production cross section and branching fraction depends on whether the decay to leptons is allowed or not. The branching fraction for the decay $W' \to t\bar{b}$ is about 3/12 (3/9) if the W' boson decay to quarks and leptons (only the decay to quarks) is allowed. The systematic uncertainty on the cross section includes components for factorization and renormalization scale, top quark mass, and parton distribution functions, and varies between about 12% at a mass of 600 GeV and 18% at a mass of 800 GeV.

TABLE I: Production cross section at NLO for a W' boson × branching fraction to $t\bar{b}$, for three different W' boson models. The production cross sections for W'_L boson interactions also include the SM s-channel contribution as well as the interference term between the two. They have been computed at leading order and scaled to NLO according to Ref. [2]. The cross sections for W'_R boson interactions differ depending on which decays of the W' boson are allowed.

W' mass	Cross section × $B(W' \to t\bar{b})$ [pb]		
[GeV]	SM+W'_L	W'_R ($\to l$ or q)	W'_R ($\to q$ only)
600	2.17	2.10	2.79
650	1.43	1.25	1.65
700	1.03	0.74	0.97
750	0.76	0.44	0.57
800	0.65	0.26	0.34

This analysis focuses on the final state topology of single top quark production where the top quark decays into a b quark and a SM W boson, which subsequently decays leptonically ($W \to e\nu$, $\mu\nu$; including $W \to \tau\nu$ with $\tau \to e\nu$, $\mu\nu$). This gives rise to an event signature with a high transverse momentum lepton and significant missing transverse energy from the neutrino, in association with two b-quark jets. The largest backgrounds to this event signature come from W+jets and $t\bar{t}$ production. We also consider SM t-channel single top quark production as a background in this search.

The theoretical W' boson production cross section is more than 15 pb for masses between 200 GeV and 400 GeV for all three models considered here [2]. The current limits on the single top quark production cross section in the s-channel are 6.4 pb [12, 13] and 13.6 pb [10] and don't depend much on whether the W boson coupling is left-handed or right-handed. Thus, W' boson

production with a decay to a top and a bottom quark is excluded in this mass region. In this analysis we therefore explore the region of even higher masses.

The analysis utilizes the same dataset, basic event selection, and background modeling as the DØ single top quark search described in Ref. [12]. We select signal-like events and separate the data into independent analysis sets based on final-state lepton flavor (electron or muon) and b-tag multiplicity (single tagged or double tagged), where b-quark jets are tagged using reconstructed displaced vertices in the jets. The independent datasets are later combined in the final statistical analysis. We perform a binned likelihood analysis on the invariant mass distribution of all final state objects to obtain upper cross section limits at discrete W' mass points. We then compare these limits to the theoretical prediction and derive a lower limit on the mass of the W' boson for each of the models under consideration.

The data for this analysis were recorded with the DØ detector at the Fermilab Tevatron, a 1.96 TeV proton-antiproton collider. The DØ detector has a central-tracking system, consisting of a silicon microstrip tracker and a central fiber tracker, both located within a 2 T superconducting solenoidal magnet [19], with designs optimized for tracking and vertexing at pseudorapidities $|\eta| < 3$ and $|\eta| < 2.5$ [20], respectively. A liquid-argon and uranium calorimeter has a central section covering pseudorapidities $|\eta| \lesssim 1.1$, and two end calorimeters that extend coverage to $|\eta| \approx 4.2$, with all three housed in separate cryostats [21]. An outer muon system, at $|\eta| < 2$, consists of a layer of tracking detectors and scintillation trigger counters in front of 1.8 T iron toroids, followed by two similar layers after the toroids [22].

The analysis uses data recorded between August 2002 and March 2004 (230 ± 15 pb^{-1} of integrated luminosity). The data were collected using a trigger that required an electromagnetic energy cluster and a jet in the calorimeter for the electron channel, and a muon and a jet for the muon channel. The event selection follows that in Ref. [12], except that only events with two or three jets are allowed; four-jet events are excluded to reduce the background contribution from $t\bar{t}$ production.

In the electron channel, candidate events are selected by requiring exactly one isolated electron (based on a seven-variable likelihood) with transverse energy $E_T > 15$ GeV and $|\eta_{\rm det}| < 1.1$. In the muon channel, events are selected by requiring exactly one isolated muon with transverse momentum $p_T > 15$ GeV and $|\eta_{\rm det}| < 2.0$. For both channels, the events are also required to have missing transverse energy $\not\!\!E_T > 15$ GeV. Jets are required to have $E_T > 15$ GeV and $|\eta_{\rm det}| < 3.4$. Events must have exactly two or exactly three jets, with the leading jet additionally required to have $E_T > 25$ GeV and $|\eta_{\rm det}| < 2.5$. At least one of the jets is required to be b-tagged using a secondary-vertex algorithm [23]. We separate the dataset into orthogonal subsets based on whether one or two jets are b-tagged.

We estimate the acceptances for W' boson production of single top quarks using events generated by the CompHEP 4.4.3 matrix element event generator [18]. The same program is also used to estimate the yield for the SM single top quark background. Interference between the SM s-channel and W'_L boson production is taken into account in the CompHEP event generation for left-handed couplings. The W' boson signals are normalized to the NLO cross section from Table I, and we use the CTEQ6L1 parton distribution functions [24].

We use both Monte Carlo and data to estimate the other background yields. The W+jets and diboson (WW and WZ) backgrounds are estimated using simulated events generated with ALPGEN [25]. The diboson background yield is normalized to NLO cross sections computed with MCFM [26]. The fraction of heavy-flavor ($Wb\bar{b}$) events in the W+jets background is determined at the parton level, using MCFM with the same parton-level cuts applied as for the samples used in the simulation. The overall W+jets yield is normalized to the data sample before requiring a b-tagged jet. This normalization to data also accounts for smaller contributions such as Z+jets events, where one of the leptons from the Z boson decay is not reconstructed. The $t\bar{t}$ background is estimated using simulated samples generated with ALPGEN, normalized to the (N)NLO cross section calculation: $\sigma(t\bar{t}) = 6.7 \pm 1.2$ pb [27]. The background due to SM t-channel single top quark production is normalized to the NLO cross section calculation: $\sigma(tqb) = 1.98 \pm 0.32$ pb [14]. When investigating the right-handed W' boson coupling, the SM s-channel is also added as a background. The uncertainty on the top quark mass is taken into account in the cross section uncertainty. The parton-level samples are then processed with PYTHIA 6.2 [28] and a GEANT [29]-based simulation of the DØ detector, and the resulting lepton and jet energies are further smeared to reproduce the resolutions observed in data. Both the shape and the overall normalization of the multijet background is estimated from data, using multijet data samples that pass all event selection cuts but fail the electron likelihood requirement in the electron channel or the muon isolation requirement in the muon channel. The simulated signal and background samples include not only the decays $W \to e\nu, \mu\nu$, but also the small contribution from $W \to \tau\nu$ with $\tau \to e\nu,\ \mu\nu$.

The large mass of the W' boson sets it apart from all background processes, hence the best place to look for such a particle is the distribution of the reconstructed invariant mass in the resonance production process. We reconstruct the invariant mass of the W' boson (the invariant mass of all final state objects $\sqrt{\hat{s}}$) by adding the four-vectors of all reconstructed final state objects: the jets, the lepton, and the neutrino from the W boson decay from the top quark decay. The xy-components of the neutrino momentum are given by the missing transverse

energy. The z-component is calculated using a SM W boson mass constraint, choosing the solution with smaller $|p_z^\nu|$ from the two possible solutions. In order to isolate the W' boson signal, we require $\sqrt{\hat{s}} > 400$ GeV.

Figure 3 shows a comparison of the invariant mass distribution in data to the sum of all background processes. Also shown are the expected contributions for W' bosons with left-handed and right-handed couplings at three different masses.

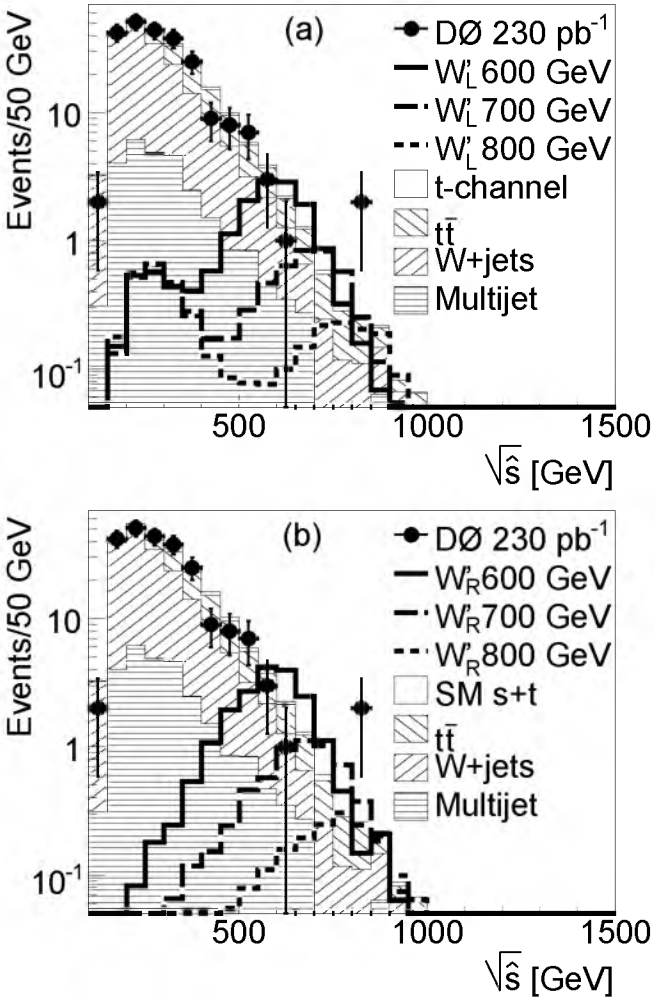

FIG. 3: The reconstructed W' boson invariant mass for several different W' boson masses as well as background processes for (a) left-handed W' boson couplings, and (b) right-handed couplings when only the decay to quarks is allowed. Electron, muon, single-tagged, and double-tagged events are combined.

The observed event yield is consistent with the background model in every bin within uncertainties. There are two events at an invariant mass of more than 800 GeV, with an expected background of about 0.5 events. This excess of events is consistent with an upward fluctuation of the background.

Systematic uncertainties are evaluated for the simulated signal and background samples, separately for electrons and muons and for each b-tag multiplicity. The dominant sources of systematic uncertainty on the signal and background acceptances are (a) the uncertainty on the b-tag modeling in the simulation, (b) the uncertainty from the jet energy scale, (c) 5% uncertainty on the object identification efficiencies, (d) 5% uncertainty on the trigger modeling, and (e) 5% uncertainty on the modeling of jet fragmentation [13]. Each of these systematic uncertainties has been evaluated by varying the uncertainty for each object in the event (electrons, muons, jets) up and down by one standard deviation, and then propagating the updated objects and corresponding weights through the analysis chain. The uncertainty on the integrated luminosity is 6.5%. The background yields also have uncertainties from the cross sections, which vary from 8% for diboson production to 15% for SM t-channel single top quark production and 18% for the $t\bar{t}$ samples [27]. Since the W+jets background is normalized to the data before tagging, the yield estimate is mainly affected by uncertainties related to b-tagging. These include the b-tag modeling uncertainty, and the uncertainty in the flavor composition before tagging derived from MCFM, which is estimated at 25%. The W+jets background yield estimate also has an uncertainty component from the parton level modeling of the $\sqrt{\hat{s}}$ distribution, which we estimate as 10% based on event yield comparisons in the sample before requiring a b-tag. The uncertainty in the background yield due to the jet energy scale varies between 15% and 30% for the single top, top pair, and diboson background samples. The uncertainty is large in these samples because most events have a small invariant mass and only very few events are in the region $\sqrt{\hat{s}} > 400$ GeV. Changing the jet energy by a small amount doesn't change the overall distribution very much, but it has a large impact on the number of events in the region $\sqrt{\hat{s}} > 400$ GeV. The uncertainty from b-tag modeling is about 8% in the single-tagged sample and about 20% in the double-tagged one. The total uncertainty on the multijet samples is large ($\approx 35\%$) due to the small number of events in the data sample used to model this background.

Due to their similar kinematic properties, the W' boson signal processes all have very similar systematic uncertainties. The overall yield uncertainty due to the jet energy scale is small (1–2%) for the signal processes because most of the signal events are in the region $\sqrt{\hat{s}} > 400$ GeV. The overall yield uncertainty for the signal samples has significant contributions from b-tag modeling (4% for the single-tagged, 16% for the double-tagged sample) and trigger modeling. The uncertainty in the signal region is significantly larger. For example, the yield uncertainty due the jet energy scale for a cut of $\sqrt{\hat{s}} > 600$ GeV is about 40% for the W'_R (600 GeV) sample.

Table II shows the event yield in the region $\sqrt{\hat{s}} > 400$ GeV for all samples, including the total systematic

uncertainty. The uncertainty includes both acceptance and normalization components.

TABLE II: Event yields with uncertainty after selection, for the electron and muon channel, single-tagged and double-tagged samples combined, after event selection and requiring $\sqrt{\hat{s}} > 400$ GeV. The W+jets row also includes diboson backgrounds. The total uncertainty on the background sum takes correlations between different backgrounds into account.

	Event Yields for $\sqrt{\hat{s}} > 400$ GeV		
	SM+W'_L	W'_R ($\to l$ or q)	W'_R ($\to q$ only)
Signals			
W' (600 GeV)	13.0 ±2.3	13.8 ±2.4	18.4 ±3.2
W' (650 GeV)	7.1 ±1.3	7.9 ±1.1	10.4 ±1.5
W' (700 GeV)	4.4 ±0.8	4.6 ±0.8	6.0 ±1.1
W' (750 GeV)	2.4 ±0.4	2.6 ±0.5	3.4 ±0.6
W' (800 GeV)	1.6 ±0.3	1.5 ±0.3	1.9 ±0.4
Backgrounds			
SM t-channel		1.9 ±0.8	
$t\bar{t}$		16.9 ±5.6	
W+jets		17.8 ±4.5	
Multijet		4.4 ±1.5	
Background sum		41.0 ±10.2	
Data		30	

The observed data are consistent with the background predictions within uncertainties. We therefore set upper limits on the W' boson production cross section for several different W' boson masses in each model. We use a Bayesian approach [30] and follow the formalism given in Ref. [12]. The limits are derived from a likelihood function that is proportional to the probability to obtain the number of observed counts. Binned likelihoods are formed based on the final state invariant mass distribution, assuming a Poisson distribution for the observed counts and a flat prior probability for the signal cross section. The priors for the signal acceptance and the background yields are multivariate Gaussians centered on their estimates and described by a covariance matrix taking into account correlations across the different sources and bins.

We combine the electron and muon, single-tagged and double-tagged analysis channels. Figure 4 shows the cross section limits together with the cross sections from Table I and their uncertainties.

At the 95% confidence level, the shaded areas above the solid lines are excluded by this analysis. The intersection of the solid line with the lower edge of the uncertainty band on the predicted cross section defines the 95% confidence level lower mass limit for each model. Together with the limit from the SM s-channel single top quark search [12], we thus exclude the presence of a W' boson with SM-like left-handed coupling if it has a mass between 200 GeV and 610 GeV. We also exclude the presence of a W' boson with right-handed couplings that is allowed to decay to leptons and quarks (only quarks) if it has a mass between 200 GeV and 630 GeV (670 GeV). This is the first direct search limit for W' boson production that takes interference with the SM into account properly. It is also the most stringent limit in the top quark decay channel of the W' boson.

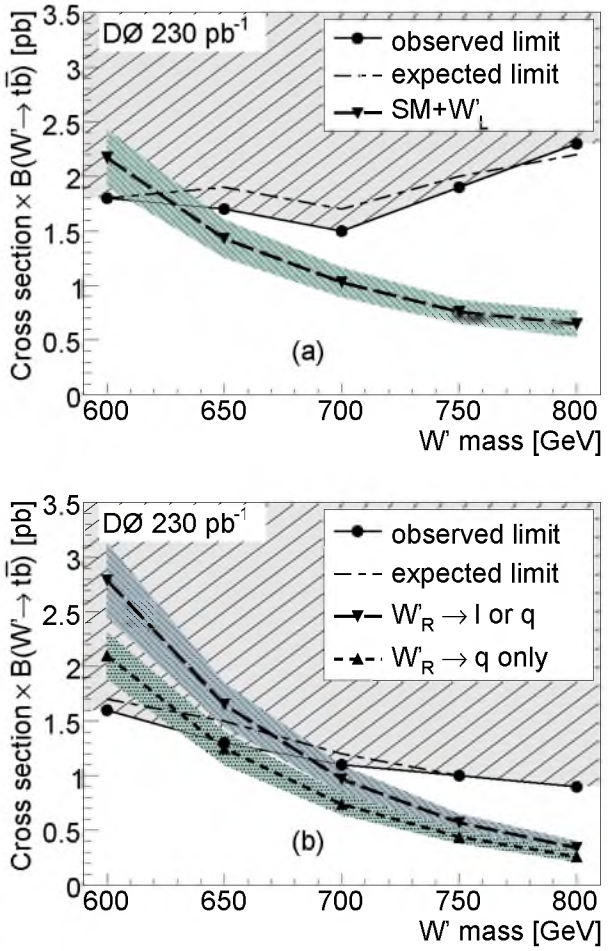

FIG. 4: Cross section limits at the 95% confidence level versus the mass of the W' boson with (a) left-handed couplings and (b) right-handed couplings. Also shown are the NLO cross sections according to Table I and the expected limits. The shaded regions above the circles are excluded by this measurement.

Acknowledgments

We are grateful to Tim Tait for discussions related to this search. We thank the staffs at Fermilab and collaborating institutions, and acknowledge support from the DOE and NSF (USA); CEA and CNRS/IN2P3 (France); FASI, Rosatom and RFBR (Russia); CAPES, CNPq, FAPERJ, FAPESP and FUNDUNESP (Brazil); DAE and DST (India); Colciencias (Colombia); CONA-

CyT (Mexico); KRF and KOSEF (Korea); CONICET and UBACyT (Argentina); FOM (The Netherlands); PPARC (United Kingdom); MSMT (Czech Republic); CRC Program, CFI, NSERC and WestGrid Project (Canada); BMBF and DFG (Germany); SFI (Ireland); The Swedish Research Council (Sweden); Research Corporation; Alexander von Humboldt Foundation; and the Marie Curie Program.

[1] T. Tait and C.-P. Yuan, Phys. Rev. D **63**, 014018 (2001).
[2] Z. Sullivan, Phys. Rev. D **66**, 075011 (2002).
[3] T. Affolder *et al.* [CDF Collaboration], Phys. Rev. Lett. **87**, 231803 (2001).
[4] J. Alitti *et al.* [UA2 Collaboration], Nucl. Phys. B **400**, 3 (1993).
[5] F. Abe *et al.* [CDF Collaboration], Phys. Rev. D **55**, 5263 (1997).
[6] V.M. Abazov *et al.* [DØ Collaboration], Phys. Rev. D **69**, 111101 (2004).
[7] D. Acosta *et al.* [CDF Collaboration], Phys. Rev. Lett. **90**, 081802 (2003).
[8] F. Abe *et al.* [CDF Collaboration], Phys. Rev. Lett. **74**, 2626 (1995); S. Abachi *et al.* [DØ Collaboration], Phys. Rev. Lett. **74**, 2632 (1995).
[9] D. Acosta *et al.* [CDF Collaboration], Phys. Rev. D **65**, 091102 (2002); D. Acosta *et al.* [CDF Collaboration], Phys. Rev. D **69**, 052003 (2004).
[10] D. Acosta *et al.* [CDF Collaboration], Phys. Rev. D **71**, 012005 (2005).
[11] B. Abbott *et al.* [DØ Collaboration], Phys. Rev. D **63**, 031101 (2001); V. M. Abazov *et al.* [DØ Collaboration], Phys. Lett. B **517**, 282 (2001).
[12] V.M. Abazov *et al.* [DØ Collaboration], Phys. Lett. B **622**, 265 (2005).
[13] V.M. Abazov *et al.* [DØ Collaboration], submitted to Phys. Rev. D, arXiv:hep-ex/0604020 (2006).
[14] B.W. Harris, E. Laenen, L. Phaf, Z. Sullivan, and S. Weinzierl, Phys. Rev. D **66**, 054024 (2002).
[15] Z. Sullivan, Phys. Rev. D **70**, 114012 (2004).
[16] J. Campbell, R.K. Ellis, and F. Tramontano, Phys. Rev. D **70**, 094012 (2004).
[17] Q.H. Cao, R. Schwienhorst, and C.-P. Yuan, Phys. Rev. D **71**, 054023 (2005).
[18] E. Boos *et al.* [CompHEP Collaboration], Nucl. Instrum. Methods A **534**, 250 (2004).
[19] V.M. Abazov *et al.* [DØ Collaboration], Nucl. Instrum. Methods A **565**, 463-537 (2006).
[20] Pseudorapidity is defined as $\eta = -\ln(\tan\frac{\theta}{2})$, where θ is the polar angle with respect to the beam axis, with the origin at the primary vertex. Detector fiducial regions are defined by detector pseudorapidity $\eta_{\rm det}$ which is calculated with the origin at the nominal center of the detector ($z = 0$).
[21] S. Abachi *et al.* [DØ Collaboration], Nucl. Instrum. Methods A **338**, 185 (1994).
[22] V.M. Abazov *et al.*, Nucl. Instrum. Methods A **552**, 372 (2005).
[23] V.M. Abazov *et al.* [DØ Collaboration], Phys. Lett. B **626**, 35 (2005).
[24] J. Pumplin *et al.*, J. High Energy Phys. **0207**, 012 (2002).
[25] M.L. Mangano *et al.*, J. High Energy Phys. **0307**, 001 (2003).
[26] J. Campbell and K. Ellis, `http://mcfm.fnal.gov`; J. Campbell and K. Ellis, Phys. Rev. D **65**, 113007 (2002).
[27] N. Kidonakis and R. Vogt, Phys. Rev. D **68**, 114014 (2003).
[28] T. Sjöstrand *et al.*, arXiv:hep-ph/0108264 (2001).
[29] R. Brun *et al.*, CERN Program Library Long Writeup W5013 (1994).
[30] I. Bertram *et al.*, FERMILAB-TM-2104 (2000).